Evaluation of dipole moments of indole derivative (5-MPIC) by Solvatochromic shift method

To cite this article: Sulochana Devar *et al* 2022 *IOP Conf. Ser.: Mater. Sci. Eng.* **1272** 012028

View the article online for updates and enhancements.

Evaluation of dipole moments of indole derivative (5-MPIC) by Solvatochromic shift method

Sulochana Devar[1*], Vijayalaxmi Gangadharmath[1], N G Yernale[2], B S Mathada[3], Omnath Patil[1] and S M Hanagodimath[1*]

[*1] Department of Physics, Gulbarga University, Kalaburagi, Karnataka, India
[2] Department of Chemistry, Guru Nanak First Grade College, Bidar, Karnataka, India
[3] PG Department of Chemistry, Organic Chemistry Research Lab, Vijaya College, Bengaluru, Karnataka, India

Corresponding author: sulochana.devar7@gmail.com; smhmath@rediffmail.com

Abstract: The Solvatochromic technique was used to examine the solvent effects of ethyl 5-methyl-3 phenyl-1*H*-indole 2-carboxylate [5-MPIC]. Different solvents were used to record 5-MPIC's absorption and emission spectra at room temperature (300 K). The ground state and excited state dipole moments were estimated experimentally using Lippert's, Bakshiev's and Kawaski Chamma Viallet's equations. The HOMO-LUMO gap and MEP map were also estimated theoretically by using B3LYP/6-31+G (d, p) basis set of Gaussian 16 w program. Dipole moments of excited states reveal a clear polarity difference between the ground and excited states.

Keywords: Dipole moments, Solvatochromic shift, HOMO-LUMO, MEP, Indole derivative.

1. Introduction

Organic compounds' absorption and emission spectra are the topic of a number of studies. The microelectronic and geometric structure of short-lived species may be gleaned from their dipole moments, making them an useful source of information. Electronically excited compounds are important in defining their photo physical and photochemical properties [1].

Indole based compounds acts as efficient dye sensitizer solar cells [2] and has diverse application in the field of biological sciences [3-5], as chemical sensors, fluorescent probes, laser dyes and non-liner optical devices. Indole composites are used as, antimicrobial, anti-cancer, anti inflamentry, anti-anxiety, anti-depressant, rodenticides and fluorescent indicators [6-11]. DFT may be used to investigate the characteristics of a substance and explain some experimental occurrences. So theoretical research may be used to measure experimental results. We also performed DFT in this regard. There has been no research done on this sort of chemical, according to a literature review. This aroused our interest in the indole derivative 5-MPIC, which is the subject of our current study.

2. Materials and methods

The indole derivative namely ethyl 5-methyl-3phenyl-1H-indol 2-carboxylate [5-MPIC], was synthesized by using reported method [12]. For the current work, spectroscopic-grade solvents such as Toluene and Benzene, acetonitrile, 1,4-dioxane, dimethyl sulfoxide, dimethyl formamide, and tetrahydrofuran were used. The samples of 5-MPIC molecule have been prepared with concentration 1×10^{-6}M.

Experiments in various solvents at room temperature using a twin beam PG Inst.Ltd., model T-90+, UV-Visible and Hitachi F-2700 Fluorescence analyzer recorded 5-MPIC's absorption and emission frequencies in the range of 250–550 nanometers. 5-MPIC's molecular structure is depicted in figure 1.
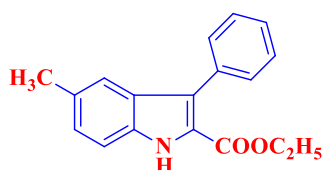

Figure1. Structure of ethyl 5-methyl-3-phenyl-1H-indole-2-carboxylate (5-MPIC)

3. Theoretical background

3.1. Evaluation of ground and excited state dipole moments

The three independent equations used for the estimation of ground and excited state dipole moments of the 5-MPICare as follows:

Lippert's equation [13]

$$\overline{\nu}_a - \overline{\nu}_f = m_1 F_1(\varepsilon, n) + \text{Constant} \tag{1}$$

Bakshiev's equation [14]

$$\overline{\nu}_a - \overline{\nu}_f = m_2 F_2(\varepsilon, n) + \text{Constant} \tag{2}$$

Kawaski Chamma Vialette's equation [15,16]

$$\frac{\overline{\nu_a} + \overline{\nu_f}}{2} = m_3 F_3(\varepsilon, n) + \text{Constant} \tag{3}$$

where F_1, F_2 and F_3 are the solvent polarity parameters, which are expressed as

$$F_1(\varepsilon, n) = \left[\left(\frac{\varepsilon - 1}{2\varepsilon - 1} \right) - \frac{(n^2 - 1)}{(2n^2 - 1)} \right] \tag{4}$$

$$F_2(\varepsilon, n) = \left[\frac{(2n^2 - 1)}{(n^2 + 2)} \right] \left[\left(\frac{\varepsilon - 1}{\varepsilon + 2} \right) - \left(\frac{n^2 - 1}{n^2 + 2} \right) \right] \tag{5}$$

$$F_3(\varepsilon, n) = \left\{ \frac{1}{2} \frac{(2n^2 + 1)}{(n^2 + 2)} \left[\frac{\varepsilon - 1}{\varepsilon + 2} - \frac{n^2 - 1}{n^2 + 2} \right] + \frac{3}{2} \left[\frac{n^4 - 1}{(n^2 + 2)^2} \right] \right\} \tag{6}$$

where,

$\overline{\nu}_a$ is absorption maximum wavelength in cm^{-1}

$\overline{\nu}_f$ is fluorescence maximum wavelength in cm^{-1},

 n & ε are refractive index and dielectric constant respectively

From the equations (4) (5) and (6) graphs$\left(\overline{v}_a - \overline{v}_f\right)$versus F$_1$($\varepsilon$, n),$\left(\overline{v}_a - \overline{v}_f\right)$ versus F$_2$(ε, n) and $\frac{\overline{v}_a + \overline{v}_f}{2}$ versus F$_3$(ε, n) have been plotted respectively and the slopes m$_1$, m$_2$ & are obtained respectively, as shown below.

$$m_1 = \frac{2\left(\mu_e - \mu_g\right)^2}{hca^3} \tag{7}$$

$$m_2 = \frac{2\left(\mu_e - \mu_g\right)^2}{hca^3} \tag{8}$$

$$m_3 = \frac{2\left(\mu_e^2 - \mu_g^2\right)}{hca^3} \tag{9}$$

The dipole moments µe and µg indicate the excited-state and ground-state dipole moments of a indole molecule. The letters '**a**' denote the Onsager's cavity radius of the solute molecule, where '**h**' is Planck's constant and '**c**' is the velocity of light. Edward [17] uses the microscopic increment method to estimate '**a**' value. The following Eqs (10) and (11) are obtained by on the basis of Eqs (8) and (9)

$$\mu_g = \frac{m_3 - m_2}{2}\left[\frac{hca^3}{2m_2}\right]^{\frac{1}{2}} \text{ For } (m_3 > m_2) \tag{10}$$

$$\mu_e = \frac{m_3 + m_2}{2}\left[\frac{hca^3}{2m_2}\right]^{\frac{1}{2}} \tag{11}$$

3.2. Molecular-Microscopic Solvent polarity Parameter

H-bonding or polarisation dependency on spectral characteristics may be studied utilizing E_T^N Reichardt [18] proposed that spectral shift and E_T^N are related. Reichardt and Ravi et al. proposed the association between the Stokes shift and, E_T^N in their various theories. Accordingly, equation (12) is obtained.

$$\overline{v}_a - \overline{v}_f = 11307.6\left(\frac{\Delta\mu^2 a_D^3}{\Delta\mu_D^2 a^3}\right) E_T^N + \text{Constant} \tag{12}$$

where $\Delta\mu = 9D$ and $a_D = 6.2\text{Å}$ are the change in dipole moment on excitation. The Stokes shift versus the, E_T^N. plot slope may be used to measure the dipole moment variation ($\Delta\mu$). The resulting equation is given by Eq (13) [15].

$$\Delta\mu = (\mu_e - \mu_g) = \sqrt{\frac{m \times 81}{\left(\frac{6.2}{a}\right)^3 \times 11307.6}} \tag{13}$$

Stokes shift vs ($\overline{v}_a - \overline{v}_f$) microscopic solvent polarity E_T^N plot constructed using Eq (12). Solvent polarity parameters (E_T^N) were culled from published study to identify their microscopic equivalent values.

4. Results and Discussion

4.1. Solvent effects on absorption and fluorescence spectra

Figures 2 and 3 show the 5-MPIC absorption and emission spectra of a variety of different solvents. 310–350 nm is the absorption wavelength. Fluorescence spectra peak between 390 and 415 nm. Table 1 shows the molecule's wavenumber in various solvents. The magnitudes of Stokes shifts may differ by around 8639 cm-1 in Stokes shift. It is shown in Tables 1 and 2 that the Stokes shift undergoes a bathochromic change when the solvent polarity increases. Excited state dipole moments are bigger than ground state dipole moments, as shown in Table 4.
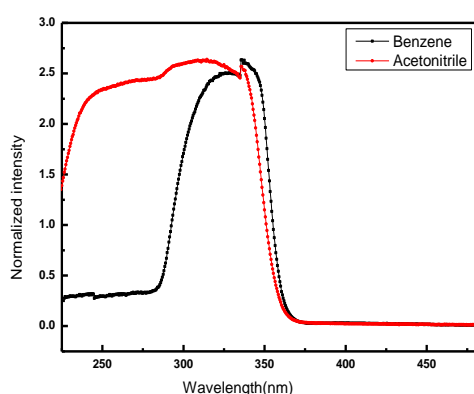
.

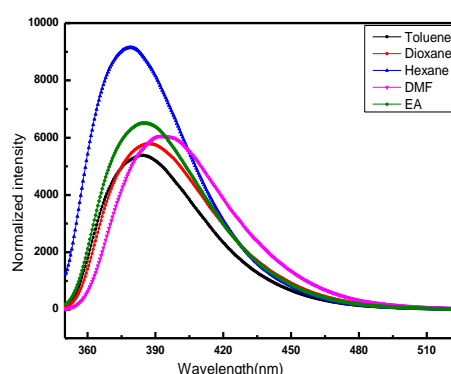**Figure 2.** Normalised absorption spectra

Figure 3. Normalised fluorescence spectra

Lippert, Bakshiev's, Kawaski-Chamma-polarity and variation of stokes shift are all shown in figures 4, 5 and 6. With regard to Stokes shift information, Viallet's functions are linear. Figure 7 shows the change in Stokes shift with the E_T^N parameter as a result of this analysis of the dipole moment. The slopes are computed in order to evaluate μg and μe. Table 3 and 4 lists the slopes, correlation factors, data points, radius, dipole moments, and change in dipole moments for 5-MPIC.
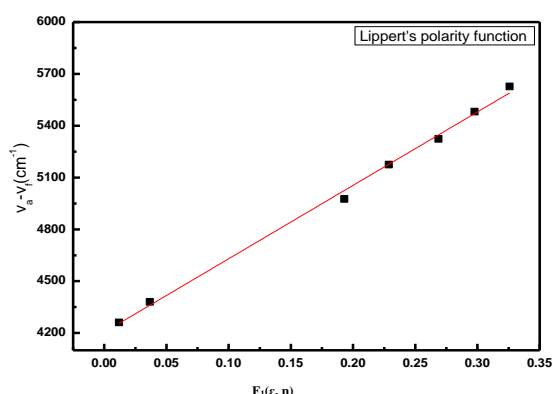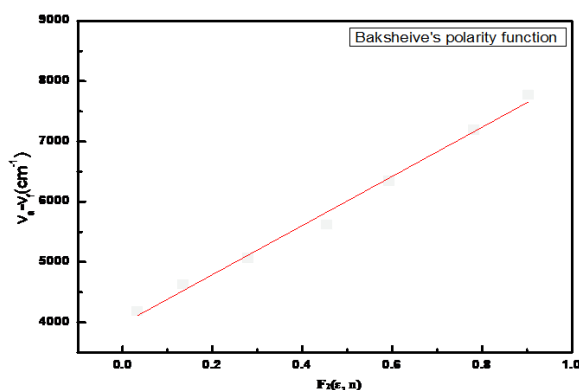

Figure 4. Lippert's polarity function

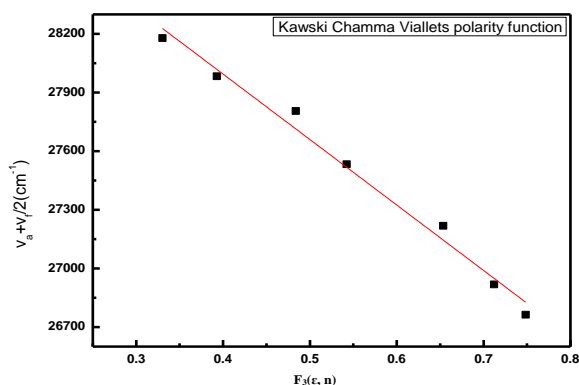**Figure 5.** Baksheives polarity function

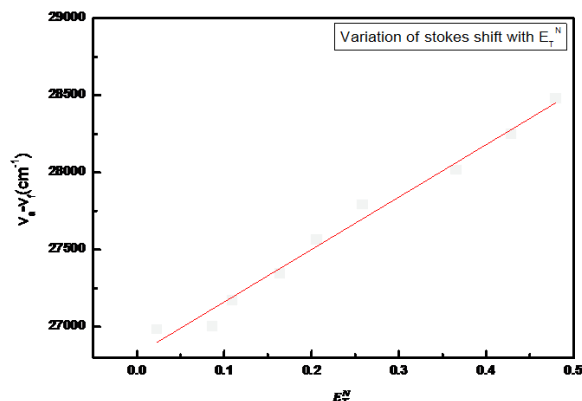**Figure 6.** Kawaski ChammaViallets polarity function

Figure 7. Variation of stoke shift with E_T^N

4.2 Analysis of quantum chemical calculation

4.2.1 Molecular orbital anlysis

As shown by HOMO and LUMO (the highest and lowest unoccupied molecular orbitals, respectively), molecular orbitals can be used to show how reactive chemical, active sites, and kinetic stability are for different molecules. HOMO represents electron giving ability of the molecule and LUMO represents electron acquisition ability. DFT/B3LYP was used to estimate the molecular orbital border based on 6-31+G (d, p). Changes in energy between these molecular orbitals are a key analytical metric in determining the transference characteristics of compounds. 3D graphs of the HOMO-LUMO gap are provided below fig 8.
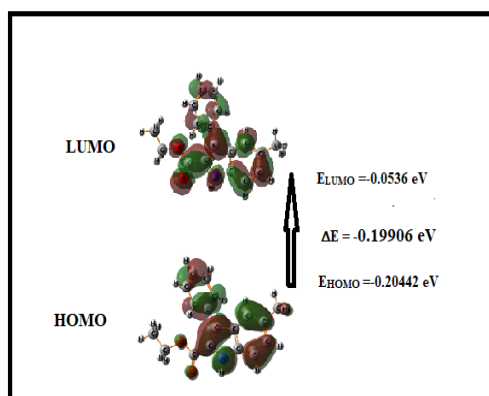
Figure 8. HOMO-LUMO Energy gap

4.2.2. Molecular electrostatic potential

Electrostatic potential maps, also known as electrostatic potential energy maps, represent the charge distributions of molecules in three-dimensional systems. In an electrophilic assault, the lowest electrostatic potential is red, while the maximum is blue in a nucleophilic attack[19-20]. The MEP of compound 5-MPIC is generated and mapped on the geometry optimisation. The colour code of MEP diagram lies between -5320.au. (Dark red) and 5320.a.u (Dark blue) for 5-MPIC.3-D mapped MEP shown in fig 9.

Figure 9. Molecular electrostatics potential map

Table1. Wavenumbers, stokes shift and arithmetic stokes shift values.

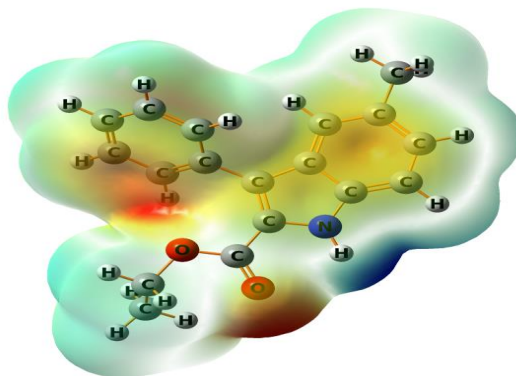| Solvents	$\overline{\nu_a}$	$\overline{\nu_f}$	$\overline{\nu_a} - \overline{\nu_f}$	$\dfrac{\overline{\nu_a} + \overline{\nu_f}}{2}$
Toluene	28571	24390	4181	26480
Benzene	28985	24096	4884	26540
Dioxane	30303	24390	5913	27346
Hexane	31250	25641	5609	28432
Cyclohexane	38461	25641	12820	32051
Acetonitrile	37037	25000	12032	31018
DMF	29411	24390	5021	26900
DMSO	30303	24350	5913	27346
EA	30303	25641	4662	27972
THF	29411	25641	3770	27526

Table 2. Polarity function and microscopic solvent polarity parameter for respective solvents.

Solvents	ε	n	F1(ε, n)	F2(ε, n)	F3(ε, n)	E_T^N
Toluene	2.40	1.497	0.015	0.033	0.744	0.099
Benzene	2.28	1.501	0.002	0.005	0.340	0.111
Dioxane	2.30	1.421	0.217	0.043	0.308	0.164
Hexane	1.80	1.370	0.010	0.242	0.346	0.006
Cyclohexane	2.02	1.426	0.001	0.002	0.289	0.006
Acetonitrile	36.64	1.344	0.305	0.861	0.665	0.46
DMF	38.25	1.430	0.275	0.839	0.711	0.386
DMSO	47	1.479	0.263	0.841	0.699	0.444
EA	6.08	1.372	0.201	0.493	0.499	0.228
THF	7.58	1.407	0.210	0.549	0.551	0.207

Table 3. Statistical treatment of the spectral shift of the compound

Compound	Slope	R square	No of data
5-MPIC	$m_1 = 12914$	0.54	7
	$m_{2} = 4259$	0.52	7
	$m_3 = -5775$	0.71	8
	$m = 3451$	0.40	9

Table 4. Onsager radius, ground and excited state dipole moments of the compound

Compound	Radius(Å)	μ_g^a(D)	μ_g^b(D)	μ_e^c(D)	μ_e^d(D)	μ_e^e(D)	μ_e^f(D)	μ_e^g(D)	μ_e^h(D)
5-MPIC	3.730	0.88	0.77	5.13	8.87	5.43	6.23	4.36	6.62

(1Debye=3.73×10^{-30}cm=10^{-18}esucm.)

[a]The ground state dipole moments using Gaussian software

[b]The ground state dipole moment calculated using equation (10)

[c]The excited state dipole moment calculated using equation (11)

[d]The excited state dipole moment calculated from Lippert's equation (7)

[e]The excited state dipole moment calculated from Bakshieves equation (8)

[f]The excited state dipole moment calculated from Kawski Chamma Viallets equation (9)

[g]The Change in dipole moment calculated using equation (10) and (11)

[h]Change in dipole calculated using equation (12)

5. CONCLUSION

For the molecule 5-MPIC, we measured the dipole moments in the ground and excited states from absorption and emission spectra by use of the Solvatochromic shift method. A larger dipole moment is detected in the excited state as compared to that of the ground state. Because the excited state is more polar than the ground state, the dipole moment increases significantly. Solavtochromic shift and microscopic solvent polarity parameter were used to compute and compare the change in dipole moment. Gaussian 16w was used to investigate theoretical ground state dipole moments, HOMO-LUMO, and MEP.

References:

1. J R Lakowicz, Principles of Fluorescence Spectroscopy, Plenum Press, 3rd ed. New York, (2006)

2. Xue-Hua Zhang, Yan Cui, Ryuzi Katoh, Nagatoshi Koumura and Kohjiro Hara *J. Phys. Chem. C* 2010, **114, 42**, 18283–18290

3. B. S. Mathada, N. G. Yernale, J. N. Basha, J. Badiger, An insight into the advanced synthetic recipes to access ubiquitous indole heterocycles, Tetrahedron Letters, Volume **85**, 2021, 153458, https://doi.org/10.1016/j.tetlet.2021.153458.

4. N.G. Yernale, B.S. Mathada, G.B. Vibhutimath, V.D. Biradar, M.R. Karekal, M.D. Udayagiri, M.B. Hire Mathada, Indole core-based Copper (II), Cobalt (II), Nickel (II) and Zinc (II) complexes: Synthesis, spectral and biological study, Journal of Molecular Structure, Volume **1248,** 2022, 131410, https://doi.org/10.1016/j.molstruc.2021.131410.

5. N. G. Yernale, B. H. M. Mruthyunjayaswamy, Metal (II) complexes of ONO donor Schiff base ligand as a new class of bioactive compounds containing indole core: Synthesis and characterization, Int J Pharm Pharm Sci, Vol **8**, Issue 1, 197-204 (2016)

6. T. Hintz, K. K. Matthews, R. Di, Biomedical Research Institute, pp.246, 2015.

7. S. Bhattacharya, J. Banerji, P.C. Ghosh, Indian J. Chem. **15**B (1977) 214.

8. N. Srividya, P. Ramasamy, V. T. Radhakrishnan, Spectrochim.Act. A, Volume **53,** pp.1743, 1997.

9. D. S. Biradar, B. Siddalingeswara, S. M. Hanagodimath, Journal of Molecular Structures, Volume **875**, pp. 108, 2008.

10. Tipperudrappa, D. S. Biradar, S. R. Manohara, S. M. Hanagodimath, S. R. Inamdar, R. J. Manekutla, Spectrochim. Act. A, Volume **69**, pp. 991, 2008.

11. R. Ghazy, S. A. Azim, M. Shaheen, F. E. Mekawey, Spectrochim.Act. A, Volume **60,** pp.187, 2004

12. S. P. Hiremath, B. H. M. Mruthyunjaya swamy, M. G. Purohit, Synthesis of substituted 2-aminoindoles and 2-(2'-phenyl-1',3',4'-oxadiazolyl) amino indoles, Indian Journal of Chemistry B, 1978, 16, 9, 789-792

13. E. Lippert, Z. Naturforsch. 10A, pp.**541**, 1955.

14. N. G. Bakhshiev, Optic Spectroscopy, (USSR) Volume **16**, pp.821, 1964.

15. L. Bilot, A. Kawski, Z. Naturforsch. 17A, pp. 621, 1962;18A, pp. 10 and 256, 1963.

16. Chamma and P. Viallet, Chemical Research Academy of. Science, Paris Ser. C, Volume **270**, pp. 1901, 1970.

17. J. T. Edward, Molecular Volumes and Parachor. Chem. Ind, London, pp. 774 (1956).

18. Reichardt, Chemical, Review, Volume**94**, pp.2319,1994

19. Gangadhar Maddapur, N R Patil, R M Melavanki, Raviraj kusnoor, Journal of Fluorescence Sep 2014

20. S Chandrashekar H R Deepa, R M Melavanki, Chemical data collection 2016